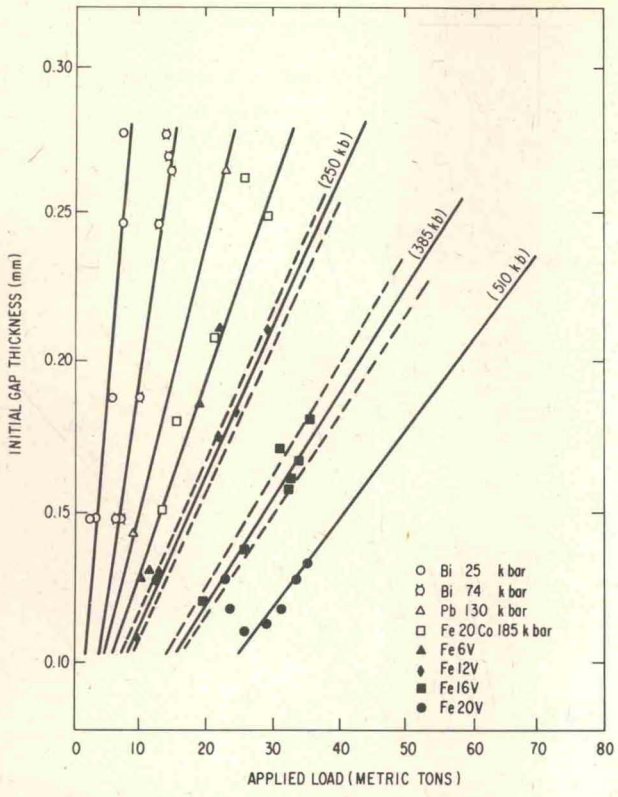

FIG. 5. Chart of G_0 vs L for the start of resistance-jump transitions of various calibration substances in the 1.37-cm-diam apparatus.

with the larger base diameter required a larger diameter cylinder and gasket, and hence, larger forces were needed to generate given face pressures.

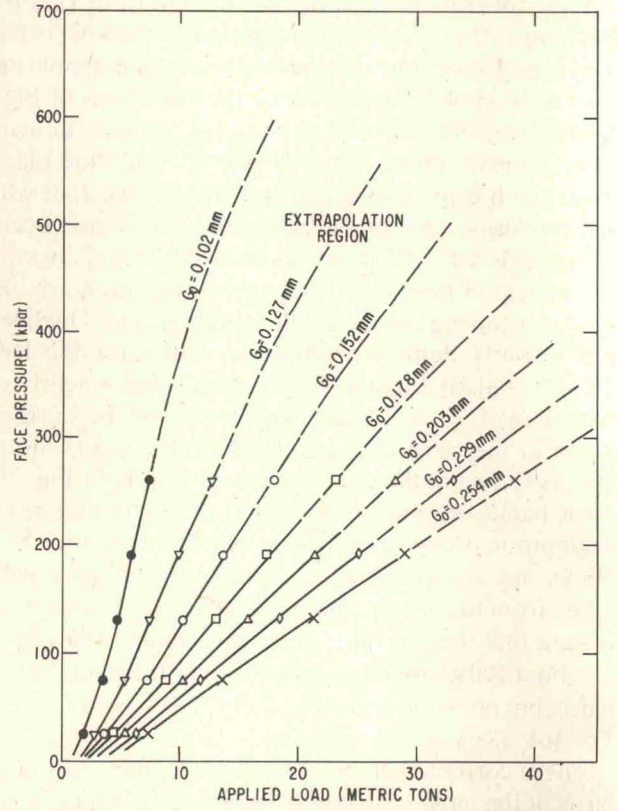

FIG. 6. P vs L, G_0 calibration chart based on well-recognized pressures below about 200–250 kilobars, and extrapolated above that.

Figure 2 shows the resistance behavior of Pb, Fe–20Co, and Fe–40Co in the 1.37-cm-diam apparatus, all at about the same initial gap conditions. For each metal there is the initial drop of resistance associated with firming up of the contacts and the cell. Then when the transition pressure is attained, the resistance increases sharply with loading until the phase transformation is complete, following which the resistance decreases slowly with increased loading. Upon unloading the reverse transition appears at much lower force loadings compared to the uploading. Because of slippage and distortion the pressure face zone does not unload at the same rate as the gasket area. This "hysteresis" behavior appears to be a common characteristic of all flank-gasketed ultrahigh pressure apparatus and is mechanical in nature. There is little reason to believe that, for a soft metal like lead, the actual pressure of the back transition is much different from that of the forward transition.

Figure 3 shows the resistance versus force loading of Fe–6V, Fe–12V, Fe–16V, and Fe–20V specimens for about the same initial gap conditions in the same apparatus. It is seen that the resistance rises associated with the $\alpha \rightarrow \epsilon$ transition are reasonably sharp, and that the usual "hysteresis" is evident in the unloading parts of the curves.

Figure 4 shows a series of experiments done in the

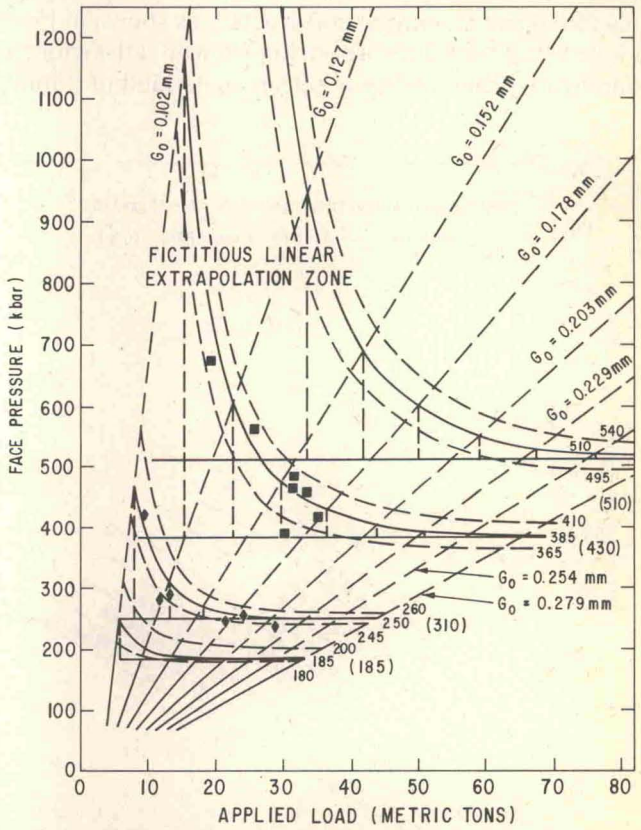

FIG. 7. Chart like Fig. 6, but ficticiously extrapolated in a linear manner. The center lines of the bands correspond to the related "Pressure lines" in Fig. 5, and the widths of the bands correspond to the widths of the data scatter bands in Fig. 5. The data points and their scatter bands are shown in Fig. 5 and Fig. 7 for the "250 kilobars" and "385 kilobars" cases. The numbers in parentheses are shock pressure values from Loree *et al.*

1.37-cm-diam apparatus with Fe–12V using different initial gaps (and hence gasket thicknesses). As mentioned above, the greater the initial gap thickness the greater the force that must be applied to the pistons to generate a given cell pressure between the faces. This is because, for the fixed taper angle of the thickness of the gasket, any change of the gap at the center changes the radial pressure distribution in the gasket. In the procedure of studying pressure calibration of the apparatus it was instructive to carry out a series of experiments for each calibration metal for a range of gaps, G_0. In this way, a family of lines could be generated on a chart showing gap versus loading force required to start the transition for each different calibrant, as shown in Fig. 5. Developing such organized sets of data is important because even with the most careful and uniform techniques of preparing and loading the cells there is some scatter of the results from the ideal functional relationship, as is evident in the chart. However, an adequate number of tests and data points establish the lines for each calibrant quite well.

II. REDUCTION OF EXPERIMENTAL DATA

If the transition pressure of each calibrant is known quite accurately in absolute terms those pressures may be assigned to the lines in Fig. 5, and from the chart a cell pressure calibration chart of P (face pressure) vs L (loading force) and G_0 may be constructed, as shown in Fig. 6. However, if the values are not known with satisfactory accuracy one can *arbitrarily* set up some kind of a formal

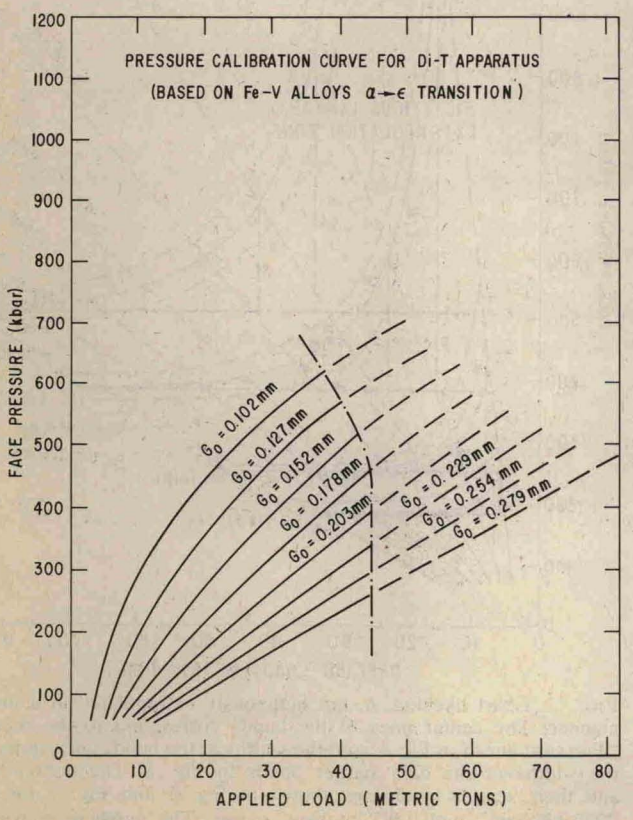

FIG. 8. Corrected, or adjusted, $P(L)$ curves for various G_0's for the 1.37-cm-diam apparatus.

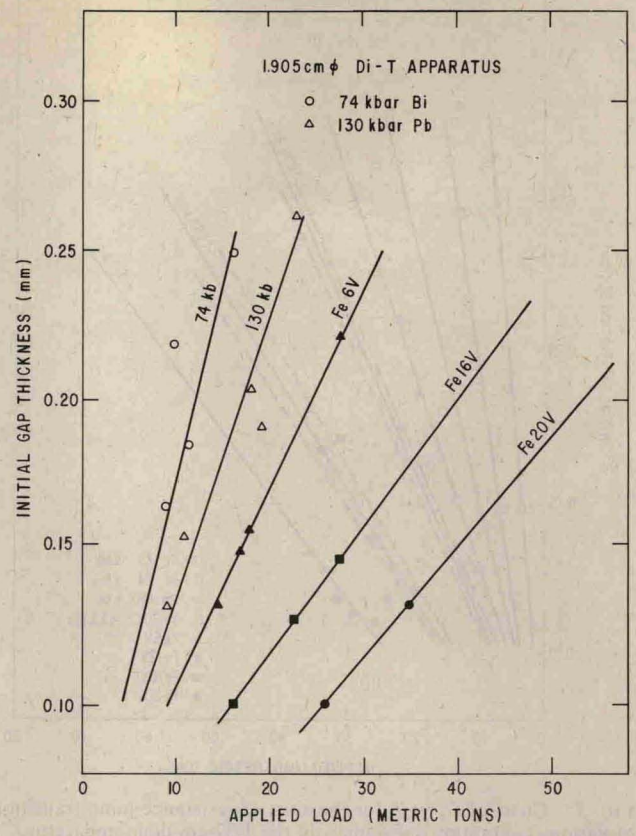

FIG. 9. Resistance-jump transition lines for various calibrants on G_0 vs L plot for the 1.905-cm-diam apparatus.

analysis procedure to develop closer probable values of the higher pressures. *One* such procedure is as follows:

First construct a chart of P vs L for various G_0's from the *lines* of Fig. 5 which correspond to the lower, fairly well established transition pressures—for example up to about 250 kilobar, as shown by the solid lines of Fig. 6. Second, extend each G_0 line linearly, (which is known to be fictitious). Third, on each extended G_0 line place a point (with error bars) corresponding to the L at which the transition of a given calibrating substance occurs. This yields a P vs L chart, as shown in Fig. 7, in which the indicated pressures for a given transition are obviously far too high at the small G_0 values, but which level out to fairly definite asymptotic values for the larger G_0's. It is likely that this asymptotic value is nearly correct, and if so, the other values should be corrected down to the same pressure level at the observed loading, as shown in the construction of Fig. 7. In Fig. 7 the error bands are indicated, and at the extreme right the asymptotic pressure transition values for the four Fe–V alloys are shown, and are compared with the values taken from the shock compression data of Loree *et al.* It is seen that there is quite good agreement of the Fe–6V (at about 190 kilobars) and the Fe–20V (at about 510 kilobars), but not so good for Fe–12V (250 vs 310 kilobars) or Fe–16V (385 vs 430 kilobars).

These corrected points for a given G_0 then become the basis of the most probable $P(L)$ curve for that G_0. Figure 8 shows the final adjusted $P(L)$ chart from the test data for the 1.37-cm-diam apparatus. The solid parts of the